PHYSICAL REVIEW B VOLUME 25, NUMBER 6 15 MARCH 1982

Shubnikov–de Haas measurements in alkali-metal–graphite intercalation compounds

M. Shayegan and M. S. Dresselhaus
Department of Electrical Engineering and Computer Science and Center for Materials Science and Engineering, Massachusetts Institute of Technology, Cambridge, Massachusetts 02139

G. Dresselhaus
Francis Bitter National Magnet Laboratory, Massachusetts Institute of Technology, Cambridge, Massachusetts 02139
(Received 9 October 1981)

Shubnikov–de Haas (SdH) oscillations are reported for well-characterized (single stage) encapsulated potassium (stages $n=4,5,8$) and rubidium ($n=2,3,5,8$) graphite intercalation compounds. Shapes of the Fermi surface (FS) are deduced from the dependence of the FS cross sections on the angle between the c-axis of the sample and $\vec{H}$. The temperature dependence ($1.4 < T \leq 25$ K) of the amplitudes of the SdH oscillations has been studied to find cyclotron effective masses for specific FS cross sections. A simple phenomenological energy-band model, based on the π bands of pristine graphite and c-axis zone folding, is used to calculate SdH frequencies as a function of Fermi energy and is applied to interpret the stage- and intercalant-dependent experimental SdH frequencies and effective masses. The good agreement between the observed and predicted effective masses and the FS cross sections confirms the general validity of this model.

I. INTRODUCTION

The most accurate determinations of the Fermi-surface (FS) parameters are carried out by measuring magneto-oscillatory phenomena such as the oscillatory magnetoconductivity Shubnikov–de Haas (SdH) effect or the susceptibility de Haas–van Alphen (dHvA) effect. Recently, these experiments have been successfully applied to a number of graphite intercalation compounds (GIC).[1–10] The interpretations of the FS cross sections have generally emphasized either the *stage dependence* or the *stage independence* of the observed SdH or dHvA frequencies (often by different groups studying the same material). The dependence or independence of the SdH frequencies on stage has significant implications on the energy-band–FS models used to interpret the experimental data. It is generally believed, however, that there is a strong similarity between the structural and electronic properties of the GIC and the parent materials (graphite and intercalant).[11] The physical basis for this relation is clear. In both graphite and the intercalant, the intralayer bonding is strong, while the interlayer bonding between graphite-graphite and intercalant-graphite layers is much weaker. In the case of dilute (high-stage) compounds, where there are several graphite layers per intercalant layer, the electronic structure is expected to be dominated by that of pristine graphite. The experimental results on the FS measurements also support the idea that the graphite π bands play a dominant role in the electronic structure of the intercalation compounds.

Stage-independent SdH-dHvA frequencies have been reported only for acceptor GIC, such as Br_2,[1,2] $SbCl_5$,[8] and $FeCl_3$.[4] The numerous frequencies (up to 11 reported[2] for Br_2-GIC) are in the range $10 \lesssim \nu \lesssim 600$ T for the above compounds. These stage-independent frequencies are generally interpreted using a metallic sandwich model proposed by Batallan *et al.*[3] and Bok *et al.*[5] It is assumed in this model that all or nearly all the charge released by the intercalate resides in the graphite bounding layers and that these layers effectively screen the charge from the interior layers. To account for the observed frequencies, these authors[2,3,5] use a nearly-free-electron model together with in-plane zone folding. Such a model, in general, predicts few frequencies and thus, in their interpretation, many of the observed frequencies are identified as harmonics or combination modes (associated with magnetic breakdown phenomena).

The SdH-dHvA frequencies observed in donor compounds[6–8] and some acceptor compounds such

as AsF_5-GIC (Refs. 9 and 10) are reported to be stage dependent. Also, not all authors agree on results for a given intercalant; for example, the recent work by Takahashi *et al.*[12] on $SbCl_5$-GIC shows stage-dependent frequencies, while the authors of Ref. 3 report stage-independent results. The stage-dependent frequencies are also numerous and, in general, the number of observed frequencies increases with increasing stage index n.[8] The simplest model used to interpret the stage-dependent frequencies is one based on the dilute-limit model (to be discussed below in some detail) proposed by McClure[13,14] and used extensively by Tanuma *et al.*[6] to interpret the dHvA frequencies observed in graphite-potassium compounds. This model, which is based on the π bands of graphite and c-axis zone folding, has also been used for the interpretation of the stage-dependent dHvA frequencies observed in acceptor compounds such as AsF_5-GIC.[9]

The structural and electronic properties of the alkali-metal GIC are among the better understood and most widely studied of all the GIC.[11,15–23] This is mostly due to the relatively simple structure of these compounds. However, there have been few reports concerning the FS measurements for these compounds.[6,7] This is perhaps partially related to the instability of the alkali-metal GIC in the presence of air and moisture, which poses difficulties in sample handling.

In this paper we report results on the angular and temperature dependence of the SdH oscillations for K-GIC (stages $n=4$, 5, and 8) and Rb-GIC ($n=2$, 3, 5, and 8). These encapsulated samples were characterized for stage index using (00l) x-ray diffractograms before and after the SdH experiments to ensure the staging fidelity of the samples during the FS measurements. The carefully handled samples showed stage- and intercalant-dependent SdH frequencies which are consistent with the results reported by Tanuma *et al.*[6] for K-GIC ($n=1$, 3, and 4). There is also numerical agreement (within experimental error of $\sim 10\%$) for the K–stage-4 compound which both groups have studied (see Table I).

In order to interpret the observed stage-dependent FS cross sections, we use two simple FS models which are based on the Slonczewski-Weiss-McClure (SWMcC) model for the π bands of graphite.[24] These two models are (I) the dilute-limit model, and (II) a general phenomenological energy-band model for GIC proposed by Dresselhaus and Leung,[25] which is a generalization of model (I). The two models are discussed briefly in Sec. III. The good agreement between the experimental results and calculated values for the FS cross sections and the cyclotron effective masses supports the basic validity of these models and provides strong evidence for the stage dependence of the FS for these donor compounds.

II. EXPERIMENTAL DETAILS AND RESULTS

The intercalated graphite samples were prepared from highly oriented pyrolytic graphite (HOPG) using the two-zone technique.[26] Blocks of HOPG were cut (parallel to the c axis) using a string saw, and then cleaved (perpendicular to the c axis) to obtain thin (<0.1 mm thick) samples with in-plane dimensions of either $\sim 5\times 5$ mm^2 ("square" samples) or $\sim 3\times 15$ mm^2 ("long" samples). The "long" samples were particularly suitable for the conductivity measurements and gave larger signals due to their higher resistance.

The growth process for the samples has been previously[27] described. The HOPG specimen and the alkali metal were placed at the two ends of a reaction ampoule which was then evacuated to ~ 10 mtorr and placed in a two-zone furnace. The HOPG crystal was kept at a relatively fixed high temperature ($T_g \approx 475-500$ °C) while the temperature of the alkali-metal intercalant T_i was varied. The temperature difference $\Delta T = T_g - T_i$ is the main parameter determining the stage of the samples.[8,26–28] For potassium and rubidium compounds, respectively, ΔT was in the range $100 \lesssim \Delta T \lesssim 300$ °C and $150 \lesssim \Delta T \lesssim 350$ °C to grow samples of stage index $2 \lesssim n \lesssim 8$, with larger ΔT values corresponding to higher n. The details of the reaction parameters and growth conditions are given in Ref. 8, and are consistent with those of Refs. 26–28.

The stages of the samples were determined by taking (00l) scans using a single crystal x-ray diffractometer. Molybdenum K_α radiation was used to minimize the x-ray absorption by the glass encapsulating the samples. A Si(Li) detector and a single-channel analyzer were employed to provide discrimination of the incident x-ray energy, thus permitting the identification of small concentrations of admixed stages.

In carrying out the SdH measurements, much attention was paid to the quality of the samples studied and to their stage fidelity. The SdH experiments showed that the SdH oscillations and the

TABLE I. Comparison of the experimentally measured FS cross sections for $\theta=0°$ with those calculated by models (I) and (II). Comparison is made for the Shubnikov—de Haas frequencies ν (in T). For each material the Fermi level E_F is given for each of the two models, together with the corresponding charge transfer per intercalate f_X and the carrier density contained within the carrier pockets N.

X	Stage	Parameter	Model (I)	Observed	Model (II)
Rb	2	ν (T)	255	255	255
			145	213	230
				28	19
		E_F (eV)	0.320		0.420
		f_X	0.07		0.07
		N (10^{20} cm^{-3})	2.12		2.12
Rb	3	ν (T)	405	405	405
			319	260	222
			124	170	
				35	
		E_F (eV)	0.463		0.500
		f_X	0.23		0.22
		N (10^{20} cm^{-3})	5.08		4.86
Rb	5	ν (T)	420;382	420	401
			280	294	300
			144	148	163
				24	27
		E_F (eV)	0.476		0.475
		f_X	0.37		0.32
		N (10^{20} cm^{-3})	5.32		4.52
K	4	ν (T)	354	354[a]	385
			300	276;264	260;246
			176	150;132	89;76
		E_F (eV)	0.420		0.480
		f_X	0.19		0.19
		N (10^{20} cm^{-3})	4.37		4.53
K	5	ν (T)	453;412	453;430	401
			304	290;267;243	300
			157	191;152;135	163
				24;18	27
		E_F (eV)	0.505		0.475
		f_x	0.30		0.24
		N (10^{20} cm^{-3})	5.85		4.60

[a]Frequencies for the K—stage-4 compound are in good agreement with those reported in Ref. 6 ($\nu=338$, 264, 238, 144, and 121 T) for the same compound.

corresponding FS cross sections are quite sensitive to the stage of the compounds (for a given alkali-metal intercalant), and thus extensive care was devoted to the characterization and protection of the samples. Because of the instability of the alkali-metal—GIC samples in the presence of air and moisture, sample handling (preparation for the conductivity measurements) was done in an argon-filled dry box ($\sim$1 ppm O_2 content) and x-ray diffraction profiles were taken before and after the SdH experiment to confirm that the samples were single staged and that no desorption had occurred during the FS measurements.

The four-point method was used to study the

in-plane resistance as a function of magnetic field. Since the emphasis was on the oscillatory part of the magnetoresistance (SdH effect), the anisotropy of the samples or the nonuniformity of the injected current posed no problem in using the four-point method. The leads were attached to the sample using conducting epoxy. The sample was then inserted in a helium-filled ampoule, which was sealed with stycast.

The SdH measurements were performed in the temperature range $1.4 \lesssim T \lesssim 25$ K while the magnetic field provided by a Bitter magnet was continuously swept up to ~ 15 T. The angular dependence (θ is the angle between the c axis of the sample and $\vec{H}$) was studied by rotating the sample around the direction of current I such that $\vec{I} \perp \vec{H}$ for all θ. Thus the transverse magnetoresistance was measured in all cases. Data acquisition was by computer, and digital processing of data was done to obtain a Fourier power spectrum of resistance versus $1/H$, thereby yielding the frequencies of the SdH oscillations which are directly related to the extremal FS cross sections.

Figure 1 shows (a) the SdH oscillations for a K—stage-5 compound at $T=4.2$ K and $\theta=0°$, (b) the oscillatory resistance, ρ_{osc} vs $1/H$ corresponding to the trace shown in (a) after the nonoscillatory magnetoresistance background is subtracted [by least-squares fitting a second-degree polynomial in H to the data shown in (a)], and (c) the Fourier transform (power spectrum) of ρ_{osc} vs $1/H$ shown in (b), in which the SdH frequencies ν_i are displayed.

In Fig. 2 the power spectra for K and Rb compounds are shown. The dominant SdH frequencies observed in these spectra are listed in the central columns of Table I. The spectra of Fig. 2 are clearly stage and intercalant dependent. The traces in Fig. 2 also show that the spectra (and thus the corresponding FS) are more complex for the higher-stage compounds than those for the samples of lower stage. This is expected from the predictions of the FS models used to interpret these data (see next section). Also note the existence of FS cross sections which are much larger than those for the majority electron and hole pockets of pristine graphite ($4 \lesssim \nu \lesssim 6$ T). Such large Fermi surfaces are a result of the transfer of significant charge from the (donor) intercalate layer to the graphite layers, and are responsible for the metallic properties of the graphite—alkali-metal compounds.[11]

Measurements of the angular dependence of the

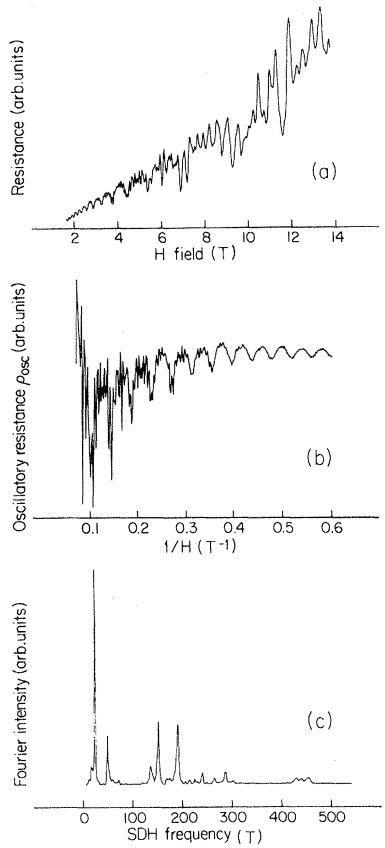

FIG. 1. Shubnikov—de Haas results for a stage-5 graphite-K sample. (a) Direct recorder trace of resistance ρ vs magnetic field H. (b) Plot of ρ_{osc} vs $1/H$, which is obtained by subtraction of the quadratic nonoscillatory background from the trace in (a). (c) The Fourier transform of the data in (b) yielding the principal frequencies contained in the Shubnikov—de Haas trace.

SdH frequencies, shown in Fig. 3 for some of the dominant frequencies of a K—stage-5 sample, suggest that the FS is largely composed of nearly cylindrical segments. A general feature of the angular dependence results (both for K and Rb compounds) is that most frequencies can not be followed to angles θ greater than $\sim 45°$ (because of the decrease in the amplitudes of the oscillations). For $\theta \lesssim 45°$, the observed frequencies follow the $\cos\theta$ curve (solid line in Fig. 3) which corresponds to a cylindrical FS. Some of the smaller frequencies, such as the 24-T frequency in Fig. 3, have significant amplitudes up to $\sim 75°$ and show deviations from cylindrical behavior. The dashed curve in Fig. 3 corresponds to an elongated ellipsoidal FS with an anisotropy ratio of 5:1. The general conclusion about the angular dependence measure-

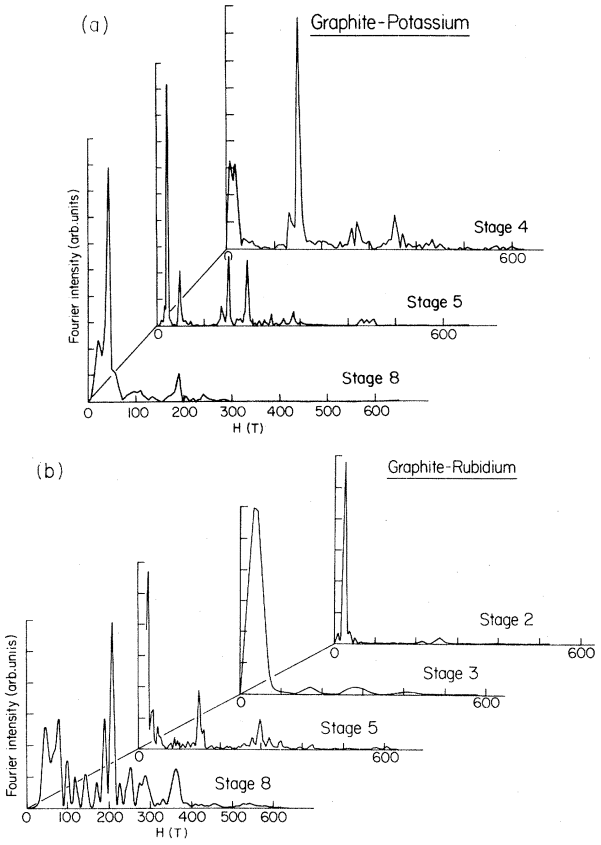

FIG. 2. Summary of the power spectra for several (a) graphite-potassium and (b) graphite-rubidium compounds, implying a dependence of the Fermi surface on stage and intercalate species.

ments is that the results are compatible with models which predict nearly cylindrical FS.

The temperature-dependent measurements were performed on a K—stage-5 sample for $4.2 \leq T \leq 25$ K at $\theta = 0°$. From the temperature dependence of the amplitudes (A) of the oscillations, the effective masses for the dominant frequencies were found. Plots of $\ln(A/T)$ vs T for several frequencies exhibit a linear temperature dependence, as shown in Fig. 4. The slopes of these lines, and the field values at which the amplitudes are measured (H_0), are used to determine the effective masses according to[29]

$$\frac{m^*}{m_0} = \frac{\ln(A/T)}{T} \frac{\hbar e}{2\pi^2 k_B m_0 c} H_0 \,. \tag{1}$$

The amplitudes of the peaks in the Fourier power spectra were also used, together with the field dependence of the amplitudes of the oscillations to yield a second determination of the effective masses.[8] The results for m^*/m_0 obtained from

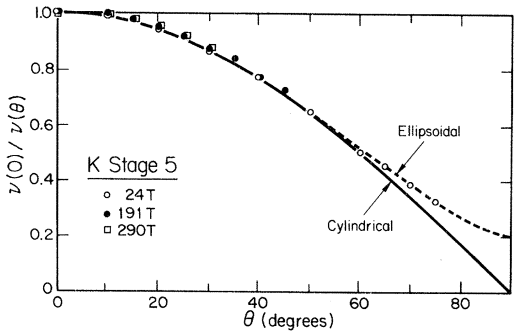

FIG. 3. The angular dependence of some of the SdH frequencies observed for a K—stage-5 sample. The normalized frequencies $\nu(0)/\nu(\theta)$ are plotted as a function of θ (angle between c axis of the sample and the H field). The experimental points for the two larger cross-section areas can only be followed for a limited range of θ and to within experimental error the points follow a cosine ($\cos\theta$) dependence (solid curve), corresponding to a cylindrical Fermi surface. The smallest cross section shows deviations from the $\cos\theta$ behavior at angles $> 60°$ and the experimental points are well represented by an ellipsoidal Fermi surface with an anisotropy ratio of 5:1 (dashed curve).

the Fourier transforms agree well (within $\sim 10\%$) with the m^*/m_0 values found from the amplitudes of the oscillations in the ρ_{osc} vs $1/H$ profiles. The observed m^*/m_0 values for the K—stage-5 compound are listed in Table II.

During the course of these studies, a great deal of care was given to ensure the reliability and reproducibility of the data. For this reason, the

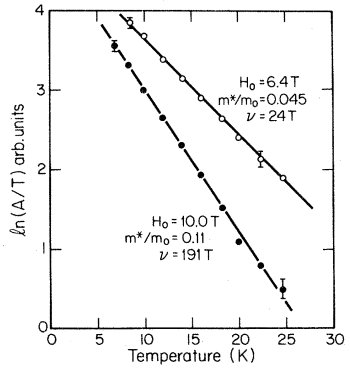

FIG. 4. Plot of $\ln(A/T)$ vs T where A is the amplitude of SdH oscillations and T is the temperature in K for the indicated SdH frequencies ν for the K—stage-5 compound. In each case the cyclotron effective-mass values are determined from the slope of the least-squares fit through the experimental points and the magnetic field H_0 at which the amplitude measurements were made.

TABLE II. Summary of observed and calculated cyclotron effective masses m^*/m_0 (in dimensionless units) for the indicated SdH frequencies for the K—stage-5 compound.

Model (I)	Observed	Model (II)
0.20 (ν=453 T)	0.15 (ν=430 T)	0.14 (ν=401 T)
0.17 (ν=304 T)	(ν=290 T)	0.12 (ν=300 T)
0.11 (ν=157 T)	0.11[a] (ν=191 T)	0.083 (ν=163 T)
	0.045 (ν=24 T)	0.051 (ν=27 T)

[a]Cyclotron effective mass m^*/m_0 observed for the ν=144 T frequency for the K—stage-4 compound in Ref. 6 is 0.075, consistent with our results.

experiment was performed on several K—stage-5 samples and on one of these, the measurements were repeated two weeks later after attaching new leads (the sample was kept in the dry box during this period). While x-ray profiles after each experimental step confirmed that the samples retained their single-stage identity, the magnetoresistance oscillations and the corresponding Fourier power spectra revealed nearly identical traces for these stage-5 compounds.[8]

Besides the single-stage samples discussed so far, the SdH measurements were made for some samples of mixed stage. In general, these were samples whose x-ray diffractograms showed a compound of stage n admixed with a small amount [a few percent, according to the integrated intensity studies of the (00l) x-ray traces] of stage $n+1$ (e.g., $n=3$ samples with admixed stage 4). For these samples, however, the x-ray profiles taken at the end of the SdH experiment showed a larger amount of stage $n+1$ present, and usually the sample had entirely transformed into stage $n+1$. These mixed-stage samples occasionally give distinct SdH frequencies, some of which could be identified with those for a stage n or $n+1$ compound.[8]

III. INTERPRETATION OF THE RESULTS

To account for the observed stage-dependent SdH frequencies, we have used two limits of the k_z-axis zone-folding model mentioned above. In model (I), the dilute-limit model,[14] the SWMcC model for the graphite π bands[24] is used, and the effect of intercalation for a stage-n donor compound is assumed to be a uniform transfer of charge from the intercalate layer to the n graphite layers, thus raising the Fermi level E_F relative to $E_F^0=-0.024$ eV for pristine graphite, where the zero of energy is taken at the H-point band extremum. The requirement that the largest predicted SdH frequency (the FS cross section at the K point) coincide with the largest observed frequency is used to determine E_F. Next, the effect of superlattice periodicity due to staging is considered, and zone folding along the k_z direction is introduced to find the extremal cross sections of the FS in the folded Brillouin zone.[30] With the trigonal warping band parameter γ_3 set equal to zero, an analytic expression[14] can be found for the FS cross section $S(\xi)$ perpendicular to the c axis as a function of ξ, the distance (in dimensionless units) from the K point along the k_z direction. The extremal FS cross sections (or FS cuts) are simply found by evaluating $S(\xi)$ at

$$\xi_i=0.5(I_c^0/I_c)i, \quad i=1,2,3,\ldots,m \tag{2}$$

where I_c^0 and I_c are the z-axis lattice constants for pristine graphite ($I_c^0=6.70$ Å) and the intercalation compound, respectively. For a compound of stage n, $I_c=(n-1)[I_c^0/2]+d_s$, where d_s is the graphite-intercalant-graphite sandwich thickness: $d_s=5.35$ Å for K, and $d_s=5.65$ Å for Rb compounds.[8,11] The largest value of i in the above expression ($i=m$) gives the smallest cross section.

In Table I the results of the application of this model [model (I)] to different compounds are given. From the values of E_F (determined as explained in the above paragraph), the carrier concentrations (N) are found by calculating the volume within the FS. Assuming the chemical compositions $C_{10.5n}K$ and $C_{14n}Rb$, determined on similarly prepared samples by (00l) integrated x-ray intensity measurements,[31] we can also estimate the charge transfer f_X per intercalate atom ($f_X=1$ means that each K or Rb atom donates one electron to the graphite layers).

Next we apply the phenomenological model

[model (II)] due to Dresselhaus and Leung for the energy bands of GIC,[25,32] which is also based on the SWMcC Hamiltonian for the graphite π bands (expressed in the three-dimensional Fourier-expansion form). The k_z-axis zone folding is used to account for the c-axis superlattice periodicity, and a unitary transformation transforms the zone-folded matrix Hamiltonian into a layer representation. For a stage n compound, n graphite layers are retained and the $(n+1)$st layer is replaced, as a first approximation, by an empty intercalate layer. The diagonalization of the Hamiltonian at a number of k points is used to obtain the electronic energy-dispersion relations which give the FS cross sections directly once the position of the Fermi energy is assumed. Again the experimental data are used to determine E_F such that the best match between the observed and calculated cross sections is obtained.

In Table I values of E_F and the resulting FS cross sections (at the K point) are listed for the "empty intercalate layer" model [under model (II)]. Because of the lack of k_z dispersion in this simplest form of the model, the resulting Fermi surfaces are very nearly cylindrical and the H-point cross sections are very close to those at the K point. Also listed in Table I are the carrier concentrations and the charge transfer for model (II) for the assumed E_F.

In order to see how the FS cross sections vary with E_F explicitly, $\ln\nu$ (ν is the SdH frequency in T) is plotted in Fig. 5 vs E_F for donor compounds ($E_F>0$). The solid lines correspond to the results of model (II) (FS cross sections at the K point) within the "empty intercalate layer" limit, while the dashed lines are the results of model (I) discussed previously. The similarity between the calculated cross sections for these two models is clear from Fig. 5. This similarity is expected because, as mentioned before, model (I) is a special case of model (II), the correspondence here being that in model (I), instead of replacing every $(n+1)$st layer of graphite by an intercalate layer (here actually by "vacuum"), the $(n+1)$st layer is a graphite layer.[33] For comparison, results of a similar analysis for acceptor compounds ($E_F<0$) are shown in Fig. 6.

From the slopes of the cross section curves in Fig. 5 one can find the cyclotron effective mass at the Fermi level defined by

$$m^* = \frac{\hbar^2}{2\pi}\frac{dA}{dE}\bigg|_{E_F}. \tag{3}$$

The calculated values of m^* for the K—stage-5 compound using the E_F values in Table I are listed in Table II.

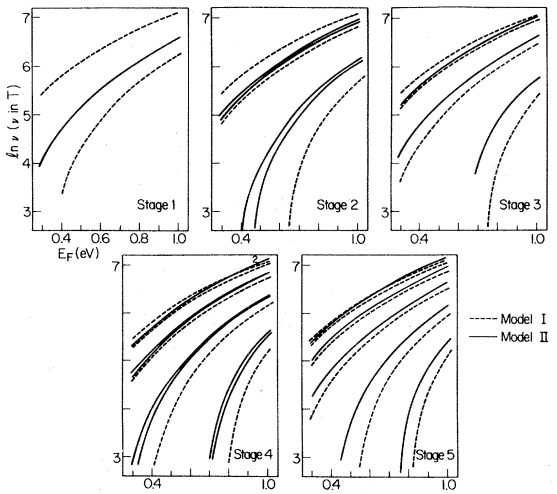

FIG. 5. Plot of $\ln\nu$ (where ν is the SdH frequency in T) vs Fermi level E_F for donor compounds with stages $1\le n\le 5$ for the two models discussed in the text. These plots are used to obtain a set of predicted Shubnikov—de Haas frequencies for a given Fermi energy. The higher frequencies are unresolved in some cases and the index 2 in the figure denotes an approximate double degeneracy. The I_c values used are for the potassium compounds ($d_s=5.35$ Å).

Excellent agreement is found between the observed and calculated [especially by model (II)] effective masses (Table II). The agreement is also

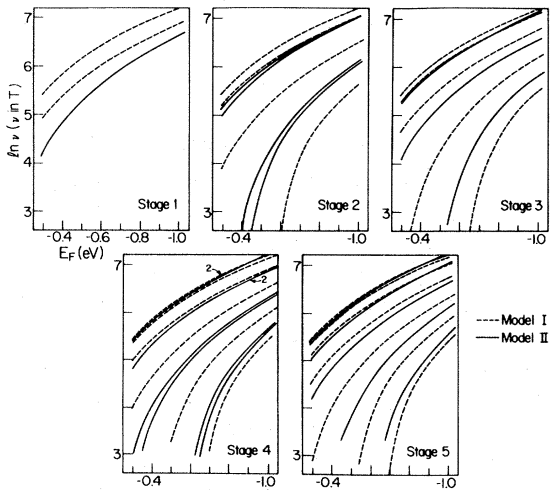

FIG. 6. Plot of $\ln\nu$ vs E_F for acceptor compounds for the two models discussed in the text (see caption to Fig. 5). The I_c values used here are for $SbCl_5$ compounds with $d_s=9.40$ Å.

good for the observed and calculated SdH frequencies for all the compounds studied [again particularly for model (II)]. A comparison of the SdH frequencies and effective masses obtained by Tanuma *et al.*[6] is given in Tables I and II for a K—stage-4 compound, the only compound measured by both groups. The good agreement between the two sets of measurements is worthy of note.

It must be emphasized that except for the known band parameters of pristine graphite, there are no additional parameters that are used in these models (except for the choice of E_F by fitting to the SdH data). Because of these simplifications it is not expected that either of these models would give an accurate quantitative fit to the experimental data. However, improvements in both models are possible. In model (I), introduction of a nonzero potential with the c-axis superlattice perodicity will cause gaps to open at the FS cuts,[30] which will give rise to new FS extremal areas slightly shifted from those calculated here. Model (II) has even more options for refinement. The introduction of an intercalant-graphite bounding-layer interaction and an intercalant-intercalant interaction will give rise to more dispersion along k_z, and thus yield different extremal FS cross sections at the K and H points (and perhaps intermediate k_z values as well). Such dispersion could explain the presence of numerous frequencies, as is observed for various compounds (especially high-stage compounds) and listed in Table I. Also the interaction parameters can be chosen so that the observed frequencies will be fitted quantitatively. The conclusion is that model (II) has the capability of fitting the SdH data in detail by the addition of a few interaction parameters.

The f_X values estimated here are in general agreement with values reported for donor[6] and acceptor[9] compounds from SdH-dHvA studies. The results indicate a stage dependence for the f_X values listed in Table I, with larger values of f_X corresponding to higher-stage compounds. This implies that the intercalant atoms are more fully ionized in the more dilute compounds. It is noted, however, that these values for f_X are relatively small (especially for the low-stage compounds). Such small f_X values may be due to the presence of other carrier pockets elsewhere in the zone whose contribution to f_X has not been included. Such carrier pockets are evidently not observed in the SdH measurements, possibly because of their heavy mass or rapid scattering.

Various other assignments of frequencies to FS cross sections have also been considered in the present work. For example, the assumption of $f_X=1$ results in certain predicted frequencies and masses, if only carrier pockets along the Brillouin-zone edges are considered. Another possible assignment results from adjusting E_F so that the largest observed frequency coincides with the second largest predicted frequency. Both of these cases were considered[8] for all the compounds that were measured, and no agreement was found either for the SdH frequencies nor for the effective masses.[8]

In addition to the results given in Table I, the above models were also applied to stage-8 compounds.[8] Both the experimental spectra (Fig. 2) and the application of the models indicate a complicated FS. Reasonable qualitative agreement is found for the SdH frequencies, but because of the great number of frequencies involved, the agreement is not quantitative. It should also be noted that for such dilute compounds, there tends to be a higher degree of admixture of regions with secondary stages, thereby complicating the experimental traces.

In general, the graphite—alkali-metal compounds of low stage have simpler physical and electronic structures (than those with high stage) and thus are more appropriate for a quantitative study. However, they are also more unstable (compared to alkali-metal—GIC samples of stage $\gtrsim 5$), and hence are more difficult to study from an experimental point of view.

Despite these limitations, the alkali-metal compounds are the graphite intercalation compounds that are most easily prepared experimentally and most easily modeled theoretically. They are also the systems which are most amenable to first-principles calculations. Several first-principles calculations on the electronic structure[18,19,22,23] and Fermi surface[18,19,23] of these materials have been completed and others are in progress. However, most of these calculations are for stage-1 compounds which were not measured in the present work. Thus careful experiments and their interpretation by phenomenological models[20,21,25] provide a critical test for first-principles calculations and will increase our fundamental understanding of the electronic structure of graphite intercalation compounds.

In the present work we have interpreted our results in terms of a three-dimensional model by Dresselhaus and Leung which emphasizes k_z-axis zone folding.[25] The phenomenological models of

Blinowski *et al.*[21] and Holzwarth[20] have many common features with the Dresselhaus-Leung model.[25] The Blinowski model however emphasizes the two-dimensional aspects of the graphite layers, including in-plane zone folding, while Holzwarth treats the graphite layers with a three-dimensional model, also emphasizing in-plane zone folding. Neither the Blinowski nor the Holzwarth models treats the c-axis periodicity explicitly. We believe the k_z-axis periodicity is the most important aspect of the basic phenomenological model and it is for this reason that the Dresselhaus-Leung model was applied to the present measurements.

IV. SUMMARY

In this paper we report results of carefully executed experimental measurements on the Fermi surface of intercalated graphite. The stage- and intercalant-dependent results are successfully interpreted using a simple phenomenological model. More high-field (>20 T) measurements on low-stage ($n=1$ and 2) compounds are needed to complete the phenomenological modeling program described here and to compare these results with the first principles calculations which are now under way.

ACKNOWLEDGMENTS

We wish to thank Dr. A. W. Moore of Union Carbide for the HOPG material, Dr. L. Rubin and Dr. B. Brandt of the Francis Bitter National Magnet Laboratory for technical assistance, Dr. S. Y. Leung for valuable discussions, and Air Force AFOSR Contract No. F49620-81-C-0006 for support. The measurements were carried out at the Francis Bitter National Magnetic Laboratory, which is supported by the National Science Foundation.

[1]A. S. Bender and D. A. Young, Phys. Status Solidi B 47, K95 (1971).
[2]I. Rosenman, G. Batallan, and G. Furdin, Phys. Rev. B 20, 2373 (1979).
[3]G. Batallan, J. Bok, I. Rosenman, and J. Mélin, Phys. Rev. Lett. 41, 330 (1978).
[4]J. A. Woollam, E. Haugland, M. B. Dowell, N. Kambe, E. Mendez, F. Hakimi, G. Dresselhaus, and M. S. Dresselhaus, *Extended Abstracts of the Fourteenth Biennial Conference on Carbon,* edited by P. A. Thrower (Pennsylvania State University Press, University Park, Penna., 1979), p. 320.
[5]J. Bok, F. Batallan, and I. Rosenman, in *Proceedings of the International Conference on the Application of High Magnetic Fields to Semiconductor Physics,* edited by J. Ryan (Clarendon, Oxford, 1978), p. 48.
[6]S. Tanuma, H. Suematsu, K. Higuchi, R. Inada, and Y. Onuki, in *Proceedings of the International Conference on the Application of High Magnetic Fields in Semiconductor Physics,* edited by J. Ryan (Clarendon, Oxford, 1978), p. 85; H. Higuchi, H. Suematsu, and S. Tanuma, J. Phys. Soc. Jpn. 48, 1532 (1980); H. Suematsu, S. Tanuma, and H. Higuchi, Physica 99B, 420 (1980).
[7]G. Dresselhaus, S. Y. Leung, M. Shayegan, and T. C. Chieu, Synth. Met. 2, 321 (1980).
[8]M. Shayegan, M. S. thesis, MIT, 1981 (unpublished).
[9]Y. Iye, O. Takahashi, and S. Tanuma, Solid State Commun. 33, 1071 (1980).
[10]R. S. Markiewicz, H. R. Hart, Jr., L. V. Interrante, and J. S. Kasper, Synth. Met. 2, 331 (1980); Solid State Commun. 35, 513 (1980).
[11]M. S. Dresselhaus and G. Dresselhaus, Adv. Phys. 30, 139 (1981).
[12]O. Takahashi, Y. Iye, and S. Tanuma, Solid State Commun. 37, 863 (1981).
[13]J. W. McClure, Phys. Rev. 119, 606 (1960).
[14]M. S. Dresselhaus, G. Dresselhaus, and J. E. Fischer, Phys. Rev. B 15, 3180 (1977).
[15]*Proceedings of the Franco-American Conference on Intercalation Compounds of Graphite, La Napoule, France, 1977,* edited by F. L. Vogel and A. Herold (Elsevier Sequoia, S. A. Lausanne, Switzerland, 1977), [Mater. Sci. Eng. 31, (1977)].
[16]*Proceedings of the International Conference on Layered Materials and Intercalates, Nijmegen, The Netherlands, 1979,* edited by C. Haas and H. Myron (North-Holland, Amsterdam, 1979) [Physica 99B, (1)—(4) (1980)].
[17]*Intercalation Compounds of Graphite II,* Proceedings of the Second Conference, Provincetown, Mass., 1980, edited by F. L. Vogel (Elsevier Sequoia, S. A. Lausanne, Switzerland, 1980), Vols. 1 and 2 [Synth. Met. 2/3 (1980)].
[18]T. Ohno, K. Nakao, and H. Kamimura, J. Phys. Soc. Jpn. 47, 1125 (1979).
[19]N. A. W. Holzwarth, L. A. Girifalco, and S. Rabii, Phys. Rev. B 18, 5206 (1978); N. A. W. Holzwarth, S. Rabii, and L. A. Girifalco, *ibid.* 18, 5190 (1978).
[20]N. A. W. Holzwarth, Phys. Rev. B 21, 3665 (1980).

[21]J. Blinowski, H. H. Nguyen, C. Rigaux, J. P. Vieren, R. Le Toullec, G. Furdin. A. Hérold, and J. Mélin, J. Phys. (Paris), 41, 47 (1980); J. Blinowski and C. Rigaux, *ibid.* 41, 667 (1980).

[22]G. Volpilhac, L. Ducasse, F. Achard, and J. Hoarau, Phys. Rev. B 23, 4236 (1981).

[23]H. Kamimura, K. Nakao, T. Ohno, and T. Inoshita, Physica 99B, 401 (1980).

[24]J. C. Slonczewski and P. R. Weiss, Phys. Rev. 109, 272 (1958); J. W. McClure, *ibid.* 108, 612 (1957).

[25]G. Dresselhaus and S. Y. Leung, Solid State Commun. 35, 819 (1980); S. Y. Leung and G. Dresselhaus, Phys Rev. B 24, 3490 (1981).

[26]A. Hérold, in *Physics and Chemistry of Materials with Layered Structures,* edited by F. Lévy (Reidel, Dordrecht, Holland, 1979), Vol. 6, p. 323.

[27]C. Underhill, T. Krapchev, and M. S. Dresselhaus, Synth. Met. 2, 47 (1980).

[28]D. E. Nixon and G. S. Parry, J. Phys. D 1, 291 (1968).

[29]D. Shoenberg, in *Progress in Low Temperature Physics,* edited by C. J. Gorter (Interscience, New York, 1957) Vol. 2, p. 234.

[30]See Ref. 6 for their sketch of the FS for a stage-4 compound.

[31]S. Y. Leung, C. Underhill, G. Dresselhaus, T. Krapchev, R. Ogilvie, and M. S. Dresselhaus, Solid State Commun. 32, 635 (1979).

[32]S. Y. Leung, Ph.D. thesis, MIT, 1980 (unpublished).

[33]There is, however, an additional cross-section curve (the uppermost one) for model (I) (see for example stage-5 compounds in Fig. 5). This is a manifestation of the fact that in model (II), when we replace the intercalate layer by "vacuum," we effectively make the intercalate level disappear from the $E(\vec{k})$ picture by taking its energy to be $-\infty$. Doing this prevents this level from interaction with other levels.